The Effect of Foaming and Silica Dissolution on Melter Feed Rheology during Conversion to Glass - 14473

José Marcial, Jaehun Chun, Pavel Hrma, and Michael Schweiger
Pacific Northwest National Laboratory, Richland, WA 99352, USA

ABSTRACT

As nuclear waste glass melter feed is converted to molten glass, the feed eventually becomes a continuous transient glass-forming melt in which dissolving refractory constituents are suspended together with numerous gas bubbles. Knowledge of mechanical properties of the melter feed is crucial for understanding the feed-to-glass conversion as it occurs in the cold cap. We measured the viscosity of the feed during heating and correlated it with the independently determined volume fractions of dissolving quartz particles and the gas phase. The measurements were performed with a rotating spindle rheometer on the melter feed heated at 5 K/min starting at several different temperatures. The effect of quartz particles, gas bubbles, and compositional inhomogeneity on viscosity of the glass-forming melt was determined by fitting a linear relationship between the log of the viscosity and the volume fractions of suspended phases.

INTRODUCTION

The "cold cap" refers to a floating layer of melter feed on a pool of molten glass in a continuous glass melter. The feed (a mixture of waste with glass-forming and -modifying additives) is charged onto the cold cap, which covers 90–95% of the melt surface. The feed moves through the cold cap and undergoes chemical reactions and phase transitions until it is converted to molten glass [1,2,3].

The waste itself contains 40 to 60 elements existing as water-soluble salts, amorphous gels, and crystalline minerals. The conversion to glass proceeds over a wide range of temperatures (from ~100 to ~1100°C) spanning the formation of molten salts that react with feed solids, turning them into intermediate products and ultimately the glass-forming melt [4,5,6]. Evolved gases escape through open pores in the cold cap until ~700–800°C, but a small fraction of residual gases can be trapped in the transient glass-forming melt and cause foaming. Foams in the cold cap reduce the heat transfer from the molten glass into the cold cap, decreasing the rate of melting [7,8].

The transient melt also contains dissolving and precipitating solid particles. Understanding the physical and mechanical properties of the melter feed in its final stage of conversion to molten glass is crucial for both feed formulation and modeling the feed-to-glass conversion. Many studies have been done on the morphology and properties of foams [8,9,10,11,12,13,14] and waste glass viscosity as a function of temperature and composition [15,16], but the rheological properties of suspensions and foams during vitrification have not been rigorously examined.

In this work, we focused on the viscosity as it evolves during the feed-to-glass conversion process. Viscosity measurements were performed on reacting feed that was heat treated from room temperature to 1200°C at 5 K min^{-1}. These measurements were compared to the predicted viscosity of a continuous phase that possesses the average glass-forming melt composition. The fraction of quartz inclusions as a function of temperature was determined through X-ray diffraction (XRD) tests. The fraction of gas inclusions was determined with pellet expansion tests, thermo-gravimetric analysis (TGA), and gas pycnometry. The fractions of gas and solid (quartz) inclusions associated with the conversion progress were employed as the key variables.

DESCRIPTION OF METHODS

Table I shows the melter feed composition used in this study. As described earlier [3,16,17], the feed (called A0) was formulated to vitrify a high-alumina high-level waste to produce glass of the following composition (with mass fractions in parentheses): SiO_2 (0.305), Al_2O_3 (0.240), B_2O_3 (0.152), Na_2O (0.096), CaO (0.061), Fe_2O_3 (0.059), Li_2O (0.036), Bi_2O_3 (0.011), P_2O_5 (0.011), F (0.007), Cr_2O_3 (0.005), PbO (0.004), NiO (0.004), ZrO_2 (0.004), SO_3 (0.002), K_2O (0.001), MgO (0.001), and ZnO (0.001). This glass was designed for the Hanford Tank Waste Treatment and Immobilization Plant, currently under construction at the Hanford Site in Washington State, USA [18]. As described by Schweiger et al. [17], the simulated melter feed was prepared in the form of slurry that was dried, crushed into powder, and placed in an oven at 105°C overnight.

TABLE I. Melter feed composition for high-alumina high-level waste in g kg^{-1} glass.

Chemicals	Mass (g)
$Al(OH)_3$	367.50
H_3BO_3	269.83
CaO	60.80
$Fe(OH)_3$	73.83
Li_2CO_3	88.30
$Mg(OH)_2$	1.70
NaOH	99.53
SiO_2	305.03
$Zn(NO_3)_2 \cdot 4H_2O$	2.67
$Zr(OH)_4 \cdot 0.654H_2O$	5.50
Na_2SO_4	3.57
$Bi(OH)_3$	12.80
Na_2CrO_4	11.13
KNO_3	3.03
$NiCO_3$	6.33
$Pb(NO_3)_2$	6.17
$Fe(H_2PO_2)_3$	12.43
NaF	14.73
$NaNO_2$	3.40
$Na_2C_2O_4 \cdot 3H_2O$	1.30
Total	1349.6

The TGA (Model SDT-Q600, TA Instruments, New Castle, DE, USA) was performed to obtain the mass change over temperature for calculating the bulk density of the feed sample. The continuous-phase density (ρ_c) was measured using a Micromeritics

AccuPyc$^{™a}$ II 1340 gas pycnometer. The volumetric expansion of the feed samples was measured with cylindrical pellets as described in Ref. [19]. The volume fraction of gas phase (bubbles) was calculated from the bulk density (ρ_b), the mass change from TGA, the volume expansion, and the continuous-phase density.

For TGA, ~20 mg samples of feed were ramp heated from room temperature to 1300°C at 5 K min^{-1} in alumina crucibles. Density samples were prepared in the form of twelve dry feed samples of ~1.75 g, heat treated at a rate of 5 K min^{-1} from room temperature to temperatures from 100 to 1200°C in 100°C increments, and crushed in the WC mill. Volumetric expansion of feed samples was measured with 1.5-g cylindrical pellets pressed at 7 MPa. The pellets were ramp heated at 5 K min^{-1} from room temperature to 1000°C in a furnace outfitted with a window that allowed a viewer to capture photographic images. Samples for XRD were prepared from 10-g feed samples heat treated at a rate of 5 K min^{-1} from room temperature to temperatures ranging from 500 to 1200°C in 100°C intervals, air quenched, and ground with 5 mass% CaF$_2$ as an internal standard. Scans were performed on a Bruker D8 Advance XRD outfitted with a Cu Kα X-ray source and a LynxEye position-sensitive detector. The collection window of the solid-state detector was 3° 2θ. Scans were performed from 5 to 70° 2θ with a 0.015° 2θ step and a 0.3-s dwell.

The bulk density, ρ_b, was obtained as:

$$\rho_b = \frac{m\rho_{b0}V_0}{m_0 V}$$

Eq. (1)

where m is the sample mass and V is the sample volume, and subscript 0 indicates room temperature. TGA provided the m/m_0 values, and volumetric expansion tests provided the V/V_0 values.

Fig. 1 provides a schematic of the experimental setup for the viscosity measurement, which was performed with ~125 g samples of powder feed poured into a platinum crucible containing the spindle at the appropriate height inside the furnace. The sample was then heated at 5 K min^{-1} from room temperature to 1100°C. The measurement started when the instrument thermocouple reached 870°C. The same procedure was applied for starting temperatures 900, 930, and 990°C. The spindle was set to a constant rotation at 0.3 rpm for the 870, 900, and 930°C trials and 0.9 rpm for the 990°C trial. Data were obtained with the use of DilaSoft II software from Theta Industries. Data acquisition occurred in 6-s intervals (i.e., the viscosity was measured at every 0.5°C increment at 5 K min^{-1}).

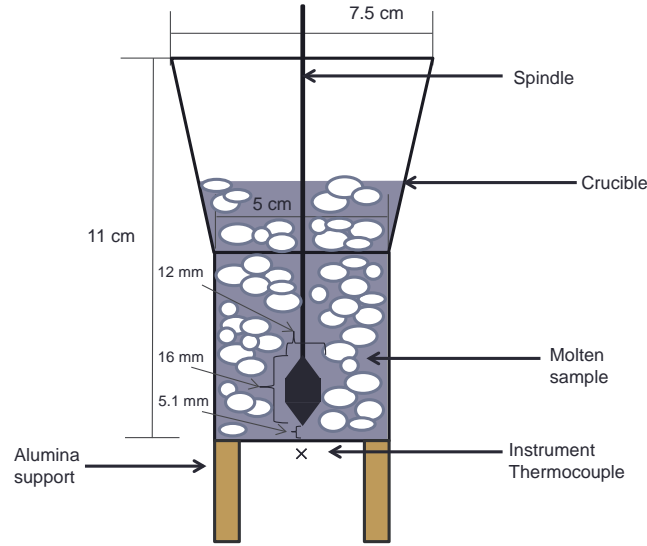[a] AccuPyc is a trademark of Micromeritics Instrument Corporation

Fig. 1. A schematic diagram of the setup for viscosity measurements

Backgrounds and Relationships For Analysis

Since $\rho_g \ll \rho_c$, where ρ_g is the gas density and ρ_c is the continuous-phase density (the melt with solid inclusions), the volume fraction of gas phase (bubbles), φ_g, is $\varphi_g = (1 - \rho_b / \rho_c)$ The density of the continuous phase was determined with a gas pycnometer.

The mass fraction of dissolved quartz was obtained by XRD and represented with an nth-order kinetic equation [20]

$$\frac{d\,x_s}{dT} = \frac{A_s}{\beta}(1 - x_s)^m \exp\left(-\frac{B_s}{T}\right)$$ Eq. (2)

where x_s is the dissolved quartz fraction ($0 < x_s < 1$), T is the temperature, A_s is the pre-exponential factor, m is the (apparent) reaction order, β is a constant heating rate ($\beta \equiv dT/dt$), and B_s is the activation energy; for 5 K min^{-1}, $A_s = 2.33$ s^{-1}, $m = 1.33$, and $B_s = 8763$ K.

The mass fraction of undissolved quartz in the melt is $g_s = g_{s0}(1 - x_s)$, where g_{s0} is the silica mass fraction in the final glass ($g_{s0} = 0.305$). The volume fraction of undissolved quartz, φ_s, is then

$$\varphi_s = \frac{1}{1 + \dfrac{\rho_s}{\rho_m}\left(\dfrac{1}{g_s} - 1\right)}$$ Eq. (3)

where ρ_s is the quartz density (2.5 g cm^{-3}) [21] and ρ_m is the melt density (with solids other than quartz) (2.6 g cm^{-3}).

The molten glass viscosity, η, is a function of temperature according to the Arrhenius equation $\eta = A\exp(B/T)$, where *A* is the pre-exponential factor (*A* = −12.51) and *B* is the activation energy for viscous flow [22]. The activation energy is a function of glass composition. For a reasonably small composition region [15,16], $B = \sum_{i=1}^{N} b_i g_i$, where b_i is the *i*th component coefficient, g_i is the *i*th component mass fraction, and *N* is the number of components [22]. Omitting minor solids, assuming that silica is the only component the glass-forming melt is lacking, and recalling that mass fractions of all components sum to 1, the activation energy of the transient glass-forming melt, B_M, is

$$B_M = \left(B_G - b_s g_{s0}\right)\frac{1 - g_s}{1 - g_{s0}} + b_s g_s \qquad \text{Eq. (4)}$$

where B_G is the activation energy of the final glass (with all quartz dissolved) and b_s is the component coefficient for SiO$_2$. Thus, the transient glass-forming melt viscosity, η_M, is

$$\eta_M = A\exp(B_M/T) \qquad \text{Eq. (5)}$$

The b_i coefficients are listed in Table II together with the glass composition used in this study. Accordingly, B_G = 1.998×10^4 K and b_s = 3.001×10^4 K.

TABLE II. Components and compositions used in this study and the corresponding viscosity coefficients used for the first-order viscosity composition model [22]

Component	Composition in the final glass, mass fraction	$10^{-4}\ b_i$ (K)
Al_2O_3	0.2407	3.506
B_2O_3	0.1522	0.352
CaO	0.0609	0.558
Fe_2O_3	0.0592	1.565
Li_2O	0.0358	−3.937
MgO	0.0012	1.184
Na_2O	0.0961	−0.031
SiO_2	0.3057	3.001
ZnO	0.0008	1.179
ZrO_2	0.0040	2.712
Bi_2O_3	0.0115	1.361
Cr_2O_3	0.0052	1.003
K_2O	0.0014	0.877
NiO	0.0040	0.397
PbO	0.0041	1.036
P_2O_5	0.0106	2.631
F	0.0067	−0.437

By Einstein's equation, viscosity of suspensions [23,24] is proportional to fractions of gaseous or solid inclusions. Here we assume that

$$\log \frac{\eta_F}{\eta_M} = f_0 + f_s \varphi_s + f_g \varphi_g \qquad \text{Eq. (6)}$$

where η_F is the reacting feed viscosity, f_s and f_g are the coefficients for solid and gaseous phase inclusions, respectively, and f_0 is the coefficient accounting for the other effects, mainly the minor solid inclusions, such as tiny crystals of spinel, and local inhomogeneities, such as the concentration layers around dissolving quartz particles (the melt within these layers has a high viscosity, whereas the viscosity of the rest of the melt is substantially lower). The η_M value was estimated for the average glass-forming melt composition, not for the melt with a high degree of local inhomogeneity. While the tiny crystals have a negligible effect on viscosity, they can influence the behavior of bubbles, which tend to grow and coalesce, because solid inclusions interfere with bubble coalescence.

By Eqs. (5) and (6)

$$\log \eta_F = A_F + \frac{B_M}{T} + f_s \varphi_s + f_g \varphi_g \qquad \text{Eq. (7)}$$

where $A_F = \log A + f_0$.

DESCRIPTION OF RESULTS

Fig. 2 shows the volume fraction of undissolved quartz, via Eq. (3), as a function of temperature. A relative volume, V/V_0, shown in Fig. 3, sharply increased by trapping evolved gases after the glass-forming melt became continuous at ~750°C) [19]. The

decrease in the volume after ~930°C is caused by the coalescence and bursting of bubbles with decreasing viscosity. Fig. 4 shows the measured density of the continuous phase as a function of temperature. Data were fit using the equation

$$\rho_c = \rho_{c0} + \rho_{c1} \tan^{-1}\left(\frac{T - T_1}{T_2}\right) + a(T - T_3)^2 \exp\left[-\left(\frac{T - T_4}{T_5}\right)^2\right]$$

Eq. (8)

where ρ_{c0} = 2492 kg m^{-3}, ρ_{c1} = 10.6 kg m^{-3}, T_1 = 534°C, T_2 = 123°C, T_3 = 100°C, T_4 = 184°C, T_5 = 389°C, and a = 5.647×10^{-3} kg m^{-3} K^{-1} are temperature-independent coefficients. The initial increase in ρ_c can be attributed to the disappearance of molten salts from the feed, whereas the decrease at higher temperatures is related to the change of materials from crystalline to amorphous. In Fig. 5 the volume fraction of bubbles as a function of temperature was calculated using Eqs. (1) and (8) with ρ_{b0} = 0.97 g cm^{-3}. Fig. 6 shows measured data for the viscosity of reacting feed.
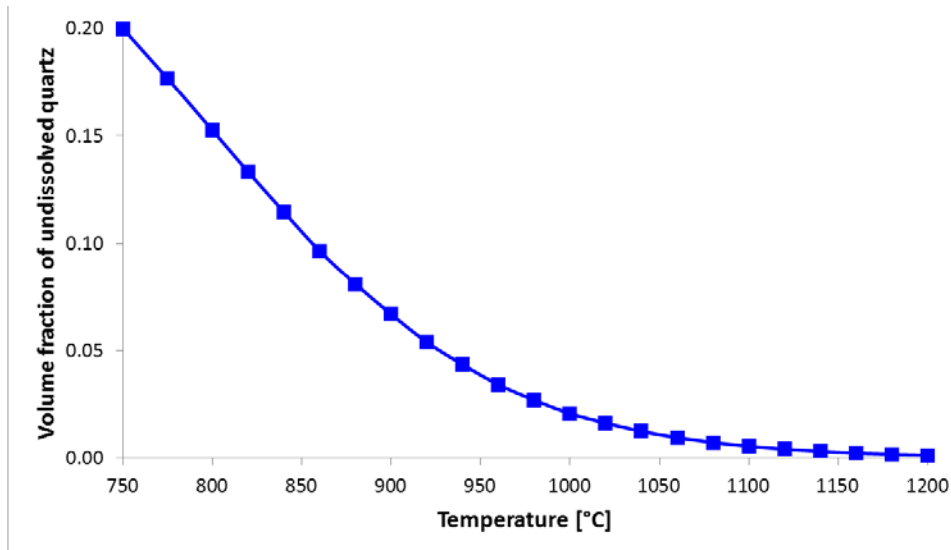

Fig. 2. Calculated volume fraction of undissolved quartz at T > 750°C from Eq. (3).
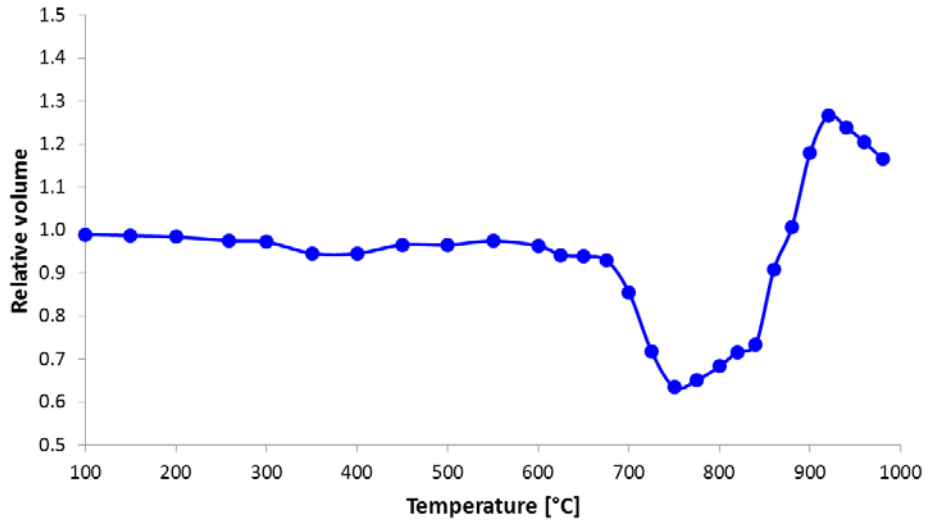
Fig. 3. Relative volume, compared to the volume at 25°C, as a function of temperature from the volumetric expansion measurements.
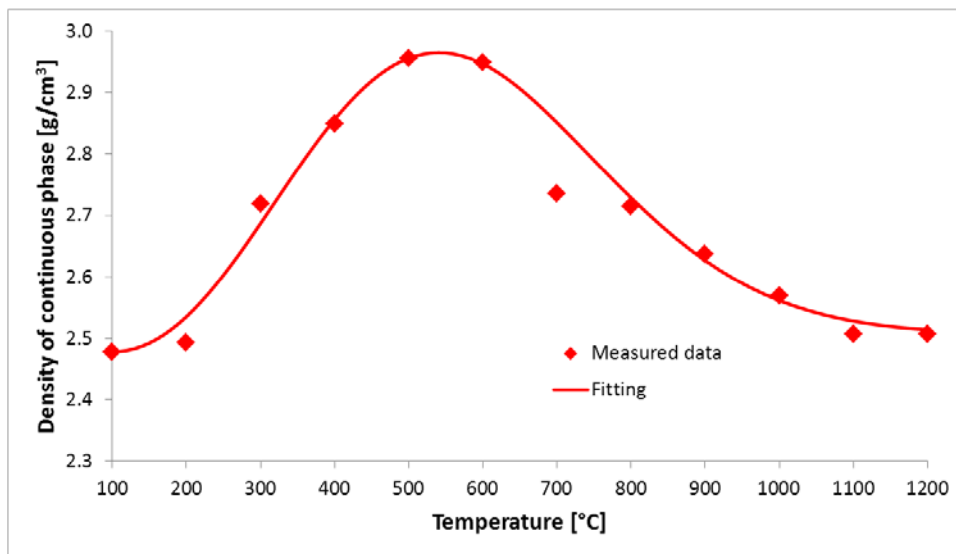

Fig. 4. Measured density of continuous phase and corresponding fitting curve.
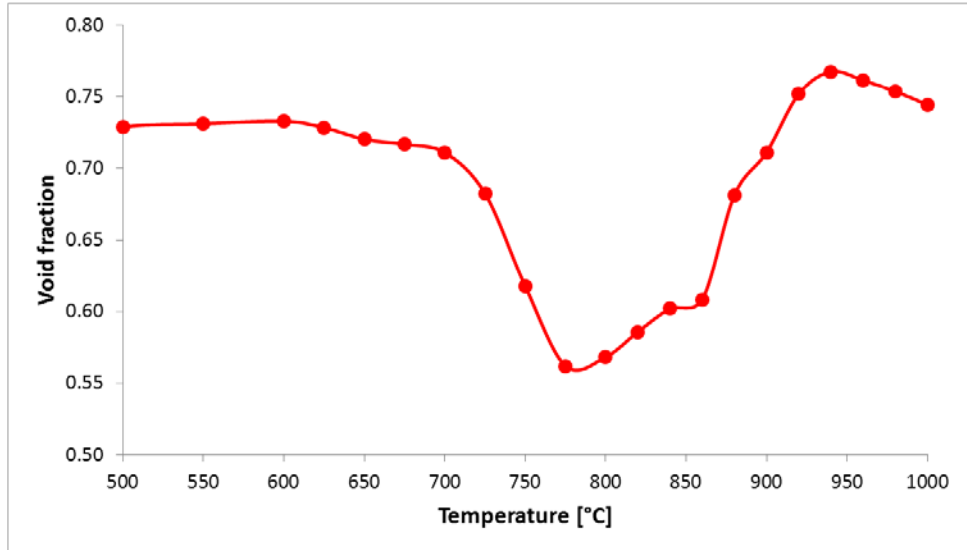
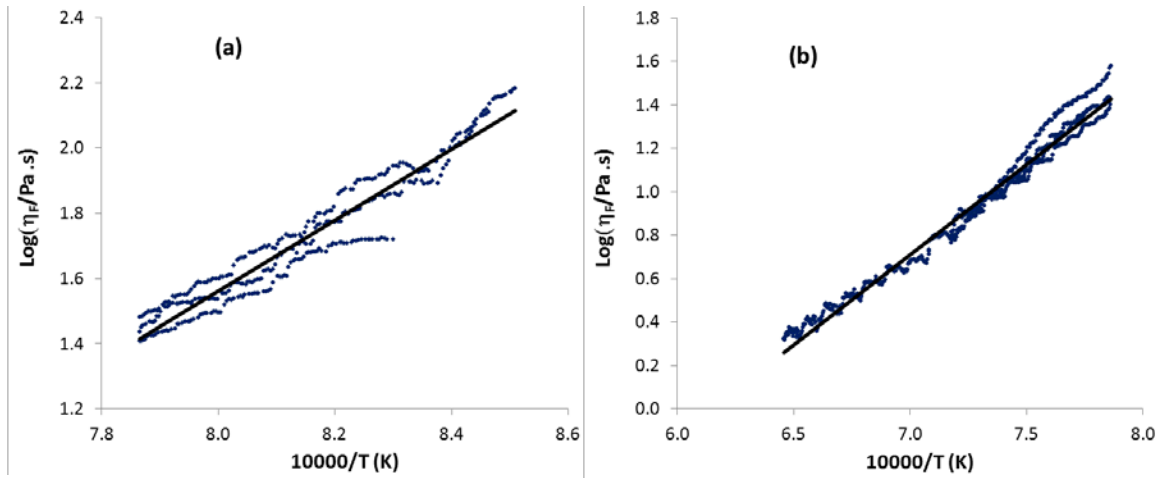Fig. 5. Void fraction as a function of temperature.

Fig. 6. Log viscosity of the foam as a function of inverse temperature (10000/T) for (a) lower ($T \le$ 1000°C) and (b) higher ($T >$ 1000°C) temperature ranges. Lines represent the fitting.

For further analysis, two separate fittings were performed at different temperature intervals:

$$\log \eta_F = -7.5936 + 1.1438 \times \left(\frac{10000}{T} \right) \text{ at } T \le 1000°C \qquad \text{Eq. (9a)}$$

$$\log \eta_F = -5.0995 + 0.8298 \times \left(\frac{10000}{T} \right) \text{ at } T > 1000°C \qquad \text{Eq. (9b)}$$

where η_F and T are in Pa s and °C, respectively.

The coefficients f_0, f_s, and f_g, obtained by fitting Eq. (6) to data, using least squares analysis applied separately for two temperature ranges ($T \leq 1000°C$ and $T > 1000°C$), are listed in Table III. Fig. 7 compares the η_F values from the measurements with Eq. (6) (the model), as well as the viscosities of the transient glass-forming melt and final glass.

TABLE III. The coefficients in the viscosity model shown in Eq. (6)

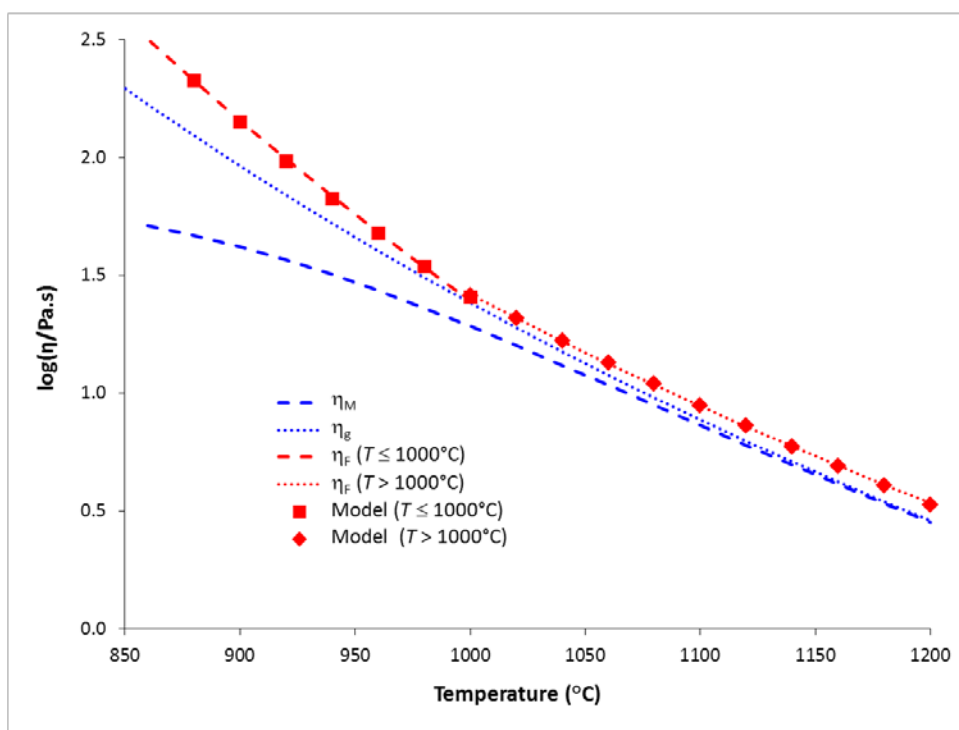| Coefficient	$T \leq 1000°C$	$T > 1000°C$
f_0	0.0	0.07
f_s	8.724	2.778
f_g	-0.0757	0.0

Fig. 7. Log viscosity of the reacting feed (η_F), the transient glass-forming melt (η_M), and the final glass (η_g) as functions of temperature.

DISCUSSION

Surprisingly, but not entirely unexpectedly, the coefficient values listed in Table III indicate that the dominant variable affecting viscosity was undissolved quartz content. The gas-phase content even shows a slight negative effect, but this effect is three orders of magnitude weaker than the effect of quartz and thus is within the experimental error. The probable cause of this puzzling result is that the quartz content and the gas content were not independent at $T < 1000°C$. This is evident for the temperature interval

10

between 800 and 950°C, where it can be shown that $\varphi_g = 0.38 + 0.45\,\varphi_s$. Further, the effect of silica-rich inhomogeneities on viscosity is closely related to the content of quartz and becomes independent only after quartz particles become small with respect to the concentration layers around them at $T > 1000$°C. Accordingly, Eq. (6) should be rewritten as

$$\log\frac{\eta_F}{\eta_M} = f_0 + f_{sg}\varphi_s \qquad\qquad \text{Eq. (10)}$$

where the subscript *sg* indicates that both undissolved quartz and gas phase jointly influence viscosity, but because φ_g and φ_s are not independent, their individual effects cannot be distinguished. Eq. (10) has the last two terms in Eq. (6) replaced by a single term $f_{sg}\varphi_s$. Note that the fraction of dissolving quartz affects melt viscosity via Eqs. (4) and (5). Using least squares analysis, we obtained $f_{sg} = 8.7$ for $T < 1000$°C and 2.8 for $T > 1000$°C.

CONCLUSIONS

The cold cap reactions produce a continuous glass-forming phase with suspended solid particles (quartz) and gas bubbles. As temperature increases and quartz particles dissolve, the glass-forming phase undergoes compositional changes. Consequently, apart from temperature, the viscosity of the reacting melter feed is affected by the presence of solid particles, gas bubbles and inhomogeneities, and by the changes in the overall composition of the liquid phase, which is a consequence of solids dissolution. A careful analysis of these effects has shown that the effect of the volume fraction of dissolving quartz is dominant and cannot be distinguished from the effect of gas bubbles because the gas phase fraction and quartz fraction are not independent.

REFERENCES

1. R. POKORNÝ and P. HRMA, "Mathematical modeling of cold cap," *J. Nucl. Mater.* 429 (2012) 245–256.
2. P. HRMA, A.A. KRUGER and R. POKORNÝ, "Nuclear waste vitrification efficiency: cold cap reactions," *J. Non-Cryst. Solids* 358 (2012) 3559–3562.
3. R. POKORNÝ, D.A. PIERCE and P. HRMA, "Melting of glass batch: Model for multiple overlapping gas-evolving reactions," *Thermochim. Acta* 541 (2012) 8–14.
4. P.A. SMITH, J.D. VIENNA and P. HRMA, "The effects of melting reactions on laboratory-scale waste vitrification." *J. Mater. Res.* 10 (1995) 2137–2149.
5. J. MATYÁŠ, P. HRMA and D.-S. KIM, *Melt Rate Improvement for High-Level Waste Glass*, PNNL-14003, Pacific Northwest National Laboratory, Richland, Washington, 2002.
6. C. RODRIGUEZ. J. CHUN, M.J. SCHWEIGER and P. HRMA, "Understanding cold-cap reactions of melter feeds through evolved gas analysis for nuclear waste vitrification." *Thermochim. Acta*, in review.

7. R.G.C. BEERKENS and J. VAN DER SCHAAF, "Gas release and foam formation during melting and fining of glass." *J. Am. Ceram. Soc.* 89 (2006) 24–35.
8. A.G. FEDOROV and L. PILON, "Glass foams: formation, transport properties, and heat, mass, and radiation transfer." *J. Non-Cryst. Solids* 311 (2002) 154–173.
9. D.J. SHAW, *Introduction to Colloid and Surface Chemistry*, Butterworths, London, 1980.
10. N.D. DENKOV, S.S. TCHOLAKOVA, R. HÖHLER and S. COHEN-ADDAD, "Foam Rheology," in: P. Stevenson (Eds.), *Foam Engineering: Fundamentals and Applications*, Wiley-Blackwell, Singapore, 2012 (Chapter 6 and Chapter 7).
11. D. WEAIRE, "The rheology of foam." *Curr. Opin. Colloid & Interface Sci.* 13 (2008) 171–176.
12. R. HÖHLER and S. COHEN-ADDAD, "Rheology of liquid foam." *J. Phys.: Condens. Matter* 17 (2005) R1041–R1069.
13. J. VAN DER SCHAAF and R.G.C. BEERKENS, "A model for foam formation, stability, and breakdown in glass-melting furnaces." *J. Colloid and Interface Sci.* 295 (2006) 218–229.
14. P. HRMA, "Effect of heating rate on glass foaming: Transition to bulk foam." *J. Non-Cryst. Solids* 355 (2009) 257–263.
15. P. HRMA, "Arrhenius model for high-temperature glass-viscosity with a constant pre-exponential factor." *J. Non-Cryst. Solids* 354 (2008) 1962–1968.
16. P. HRMA, B.M. ARRIGONI and M.J. SCHWEIGER, "Viscosity of many-component glasses." *J. Non-Cryst. Solids* 355 (2009) 891-902.
17. M.J. SCHWEIGER, P. HRMA, C.J. HUMRICKHOUSE, J. MARCIAL, B.J. RILEY and N.E. TEGROTENHUIS, "Cluster formation of silica particles in glass batches during melting," *J. Non-Cryst. Solids* 356 (2010) 1359–1367.
18. P.R. HRMA, M.J. SCHWEIGER, B.M. ARRIGONI, C.J. HUMRICKHOUSE, J. MARCIAL, A. MOODY, C. RODRIGUEZ, R.M. TATE and B. TINCHER, *Effect of Melter-Feed-Makeup on Vitrification Process*, PNNL-18374, Pacific Northwest National Laboratory, Richland, Washington, 2009.
19. S.H. HENAGER, P.R. HRMA, K.J. SWEARINGEN M.J. SCHWEIGER, J. MARCEL and N. E. TEGROTENHUIS, "Conversion of batch to molten glass, I: Volume expansion," *J. Non-Cryst. Solids* 357 (2011) 829–835.
20. R. POKORNÝ, J. A. RICE, J. V. CRUM, M. J. SCHWEIGER and P. HRMA, "Kinetic model for quartz and spinel dissolution during melting of high-level-waste glass batch." *J. Nuclear Mat.* 443 (2013) 230–235.
21. E. BOUROVA and P. RICHET, "Quartz and cristobalite: High-temperature cell parameters and volume of fusion." *Geophys. Res. Letts.* 25 (1998) 2333–2336.
22 P. HRMA and H. SANG-SOO, "Effect of glass composition on activation energy of viscosity in glass-melting-temperature range." *J. Non-Cryst. Solids* 358 (2012) 1818-1829.
23. W.B. RUSSEL, D.A. SAVILLE and W.R. SCHOWALTER, *Colloidal Dispersions*, Cambridge University Press, New York, 1989.
24. P.C. HIEMENZ and R. RAJAGOPALAN, *Principles of Colloids and Surface Chemistry*, 3rd Ed., Marcel Dekker Inc., New York, 1997.

ACKNOWLEDGEMENTS